

AD-A008 411

THE DEVELOPMENT, BUILDING, AND TESTING
OF AN ADVANCED ION MICROPROBE (AIM) ION
SOURCE SYSTEM

Richard T. Martin, et al

Applied Research Laboratories

Prepared for:

Air Force Technical Applications Center
Advanced Research Projects Agency

26 November 1974

DISTRIBUTED BY:

NTIS

National Technical Information Service
U. S. DEPARTMENT OF COMMERCE

UNCLASSIFIED

SECURITY CLASSIFICATION OF THIS PAGE (When Data Entered)

REPORT DOCUMENTATION PAGE		READ INSTRUCTIONS BEFORE COMPLETING FORM
1. REPORT NUMBER	2. GOVT ACCESSION NO.	3. RECIPIENT'S CATALOG NUMBER AD-A008411
4. TITLE (and Subtitle) FINAL REPORT: THE DEVELOPMENT, BUILDING, AND TESTING OF AN ADVANCED ION MICROPROBE (AIM) ION SOURCE SYSTEM		5. TYPE OF REPORT & PERIOD COVERED FINAL REPORT Jan. 1972 - Oct. 1974
7. AUTHOR(s) Richard T. Martin Richard D. Fralick Henry J. Roden		6. PERFORMING ORG. REPORT NUMBER
9. PERFORMING ORGANIZATION NAME AND ADDRESS Applied Research Laboratories, Inc. Hasler Research Center 95 La Patera Lane, Goleta, CA 93017		8. CONTRACT OR GRANT NUMBER (if any) F 33657-72-C-0632
11. CONTROLLING OFFICE NAME AND ADDRESS Advanced Research Project Agency (PM) 1400 Wilson Blvd. Arlington, VA 22209		10. PROGRAM ELEMENT, PROJECT, TASK AREA & WORK UNIT NUMBERS 97x0400.1302 VT/1412
14. MONITORING AGENCY NAME & ADDRESS (if different from Controlling Office) HQ USAF, AFTAC/NYR Patrick AFB, FL 32925		12. REPORT DATE 26 November
		13. NUMBER OF PAGES 47
		15. SECURITY CLASS. (of this report) UNCLASSIFIED
		15a. DECLASSIFICATION DOWNGRADING SCHEDULE
16. DISTRIBUTION STATEMENT (of this Report) Approved for public release. Distribution unlimited.		
17. DISTRIBUTION STATEMENT (of the abstract entered in Block 20, if different from Report)		
18. SUPPLEMENTARY NOTES Reproduced by NATIONAL TECHNICAL INFORMATION SERVICE US Department of Commerce Springfield, VA. 22151		
19. KEY WORDS (Continue on reverse side if necessary and identify by block number) ION MICROPROBE, ION LENSES, SPHERICAL ABERRATION, SPUTTERED ION MASS SPECTROSCOPY (SIMS).		
20. ABSTRACT (Continue on reverse side if necessary and identify by block number) An Ion Microprobe was designed, built and tested which has demonstrated primary beam spot sizes of 0.3 micron and should be capable of spot sizes of 0.1 micron. The improved spot size over previously available devices is due to greatly reduced spherical aberration in the objective lens. A secondary ion and electron collection and focusing system permits secondary ions sputtered from the sample to be transmitted to a Mass Spectrometer for analysis or permits secondary electrons from the sample to be detected for the purpose of topographical imaging of the sample in a scanning electron or scanning ion microscope mode.		

DD FORM 1473

JAN 71

EDITION OF 1964 IS OBSOLETE

UNCLASSIFIED

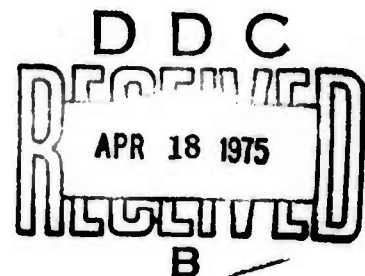
Contract No. F33657-72-C-0632
10 January 1972 (Expires 30 September 1974)
Contract Amount: \$151,968
AFTAC Project Authorization No. VT/1412/ASD Amendment 4

APPLIED RESEARCH LABORATORIES
HASLER RESEARCH CENTER
95 LA PATERA LANE, GOLETA, CALIFORNIA 93017

THE DEVELOPMENT, BUILDING, AND TESTING
OF AN ADVANCED ION MICROPROBE (AIM)
ION SOURCE SYSTEM

FINAL REPORT

26 NOVEMBER 1974



Sponsored by
Advanced Research Project Agency
ARPA Order No. 1702, Amendment No. 1
Program Code No. 2F10

Principal Investigator: Richard T. Martin (805) 967-5621
Project Scientists: Richard D. Fralick " "
Henry J. Roden " "

Neither the Advanced Research Projects Agency nor the Air Force Technical Applications Center will be responsible for information contained herein which has been supplied by other organizations or contractors, and this document is subject to later revision as may be necessary. The views and conclusions presented are those of the authors and should not be interpreted as necessarily representing the official policies, either expressed or implied, of the Advanced Research Projects Agency, the Air Force Technical Applications Center, or the U. S. Government.

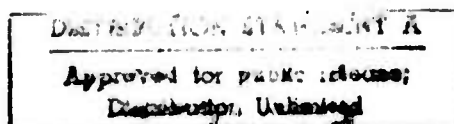


TABLE OF CONTENTS

	<u>PAGE</u>
1. SUMMARY	1
2. INTRODUCTION	3
3. FUNCTIONAL DESCRIPTION	3
4. DESIGN OF THE ADVANCED ION MICROPROBE	7
4A. DISCUSSION OF PHASE I	7
4B. RESULTS OF COMPUTER DESIGN	8
4B(1). OBJECTIVE LENS	8
4B(2). PICKUP ELECTRODE AND IMMERSION LENS	12
4C. DETAIL DESIGN	16
4C(1). SELECTION OF BASIC COLUMN CONFIGURATION	16
4C(2). PRIMARY ION SOURCE	18
4C(3). COLUMN MECHANICAL MOUNTING	20
4C(4). PRIMARY COLUMN LENSES	23
4C(5). PRIMARY ION BEAM DEFLECTION SYSTEM	25
4C(6). PRIMARY BEAM APERTURE	26
4C(7). PRIMARY BEAM CURRENT MONITOR	27
4C(8). ASTIGMATOR	28
4C(9). VISUAL OPTICS	28
4C(10). COLD DOME	29
4C(11). SECONDARY ION PICKUP ELECTRODE AND IMMERSION LENS	29
4C(12). SECONDARY ION SLIT	30
4C(13). SECONDARY ELECTRON DETECTOR	31

DISTRIBUTION STATEMENT A

Approved for public release;
Distribution Unlimited

TABLE OF CONTENTS (CONTINUED)

	<u>PAGE</u>
5. TESTING AND RESULTS	33
5A. VACUUM SYSTEM	33
5B. MECHANICAL	34
5C. ELECTRONICS	35
5C(1). HIGH VOLTAGE TESTING	35
5C(2). PRIMARY BEAM SWEEP SYSTEM	38
5D. ION TESTING	39
5D(1). PRIMARY BEAM DEFLECTION AND CURRENT MONITOR	39
5D(2). PRIMARY BEAM SPOT SIZE	40
5D(3). SECONDARY ION COLUMN AND SECONDARY ELECTRON DETECTOR	41
6. CONCLUSIONS	43
7. ACKNOWLEDGEMENT	43
8. GLOSSARY OF ABBREVIATIONS	43

TABLE AND FIGURES

		PAGE
<u>TABLE</u>		
1	TYPICAL OPERATING VOLTAGES	37
<u>FIGURES</u>		
1	TOP VIEW-ADVANCED ION MICROPROBE	5
2	COMPUTER RESULTS OF OBJECTIVE LENS DESIGN	9
3	ACTUAL MECHANICAL DESIGN OF OBJECTIVE LENS	9
4	OBJECTIVE LENS NOMINAL WORKING DISTANCE VERSUS EXCITATION RATIO	10
5	OBJECTIVE LENS FOCUS SHOWING SPHERICAL ABERRATION	11
6	VIRTUAL OBJECT CREATED BY SECONDARY ION PICK ELECTRODE FOR <u>SAME</u> POLARITY PRIMARY AND SECONDARY IONS	13
7	VIRTUAL OBJECT CREATED BY SECONDARY ION PICKUP ELECTRODE FOR <u>OPPOSITE</u> POLARITY PRIMARY AND SECONDARY IONS	14
8	SECONDARY ION PICKUP ELECTRODE CONFIGURATION SHOWING VIRTUAL OBJECT LOCATION FOR DIFFERENT BEAM POLARITIES	15
9	COMPUTER RESULT OF IMMERSION LENS DESIGN	17
10	VOLTAGE SCHEMATIC	36

1. SUMMARY

The purpose of this contract was to design and build a microfocus ion optical system which represents an order of magnitude improvement in the state-of-the-art. This system, the Advanced Ion Microprobe, is to be used as a sophisticated source system for an analytical mass spectrometer which is being designed and constructed as a joint effort of three separate laboratories.

Earlier theoretical studies suggested that it should be possible to achieve sufficient improvement in the limiting physical parameters of a microfocus ion optics system (the aberrations of the ion focusing lenses) to achieve the desired advance in performance required for the Advanced Ion Microprobe.

Computerized ion ray trace design techniques developed in the earlier studies were used to design the basic ion optic elements of the system. These theoretical designs were then transformed into realizable mechanical configurations which would accommodate the wide variety of operational requirements of the system and compatibly interface with the remaining components of the mass spectrometer system being constructed by the other laboratories. Great care was taken in the calculation and design to anticipate potential problem areas to eliminate the need for reworking and redesign. The mechanical tolerances demanded by the physics of the design were at the lower limit of available techniques and required carefully planned and executed fabrication methods.

The testing and operation of the system was done using the interfacing vacuum system and electronics from the other laboratories. Although the tests were limited in both time and ultimate level of performance due primarily to electronics difficulties, the results obtained were very encouraging.

The system displayed outstanding reliability and stability throughout the tests. The performance down to the limits imposed by the available test methods and equipment was very close to the theoretical predictions.

Primary beam spot sizes of 0.34 microns were observed on the sample with a delivered current of 2×10^{-11} amps and a density of 22 ma/cm². This measurement was made using positive ions with the ion source running on air. A theoretical estimation of the maximum possible positive ion current and current density, which considers only the deleterious effect of objective lens spherical aberration, predicts a total current of 2.78×10^{-11} amps and a density of 30 ma/cm² in a 0.34 micron spot. This same estimation predicts an ultimate spot size of about 0.05 micron with a current of 1.7×10^{-13} amps and a density of 8.5 ma/cm². In practice, the ultimate spot size will be influenced by more than just spherical aberrations and a more realistic estimate of the actual minimum spot size would be closer to 0.1 micron. When negative primary ions are used, the currents and current densities would be reduced approximately one order of magnitude.

The gas load imposed on the vacuum system by the components of the Advanced Ion Microprobe is less than that of the vacuum chamber itself and is estimated at approximately $4-5 \times 10^{-6}$ torr.liter/sec. These gas loads are sufficiently low that they should not impair the operation of the overall system.

2. INTRODUCTION

This report covers one portion of the design, construction, and testing of the Advanced Mass Spectrometer (AMS), a very large analytical mass spectrometer system. In concept the AMS is a highly sophisticated and technically advanced version of the Ion Microprobe Mass Analyzer (IMMA) sold commercially by Applied Research Laboratories. The AMS is being developed in a joint effort between Rensselaer Polytechnic Institute, General Electric's Vallecitos Nuclear Center, and Applied Research Laboratories' Hasler Research Center. The portion of the AMS developed in this laboratory is the ion optics of the mass spectrometer's source system which is called the Advanced Ion Microprobe. The Advanced Ion Microprobe requires a high vacuum chamber and pumping system, a sample stage, and considerable electronics for its operation in addition to its ion optics column. This supporting apparatus was not produced as a part of this contract but was supplied by the Vallecitos Nuclear Center.

This report discusses the function of the components which comprise the Advanced Ion Microprobe, their design, and the results of our testing of these components.

3. FUNCTIONAL DESCRIPTION

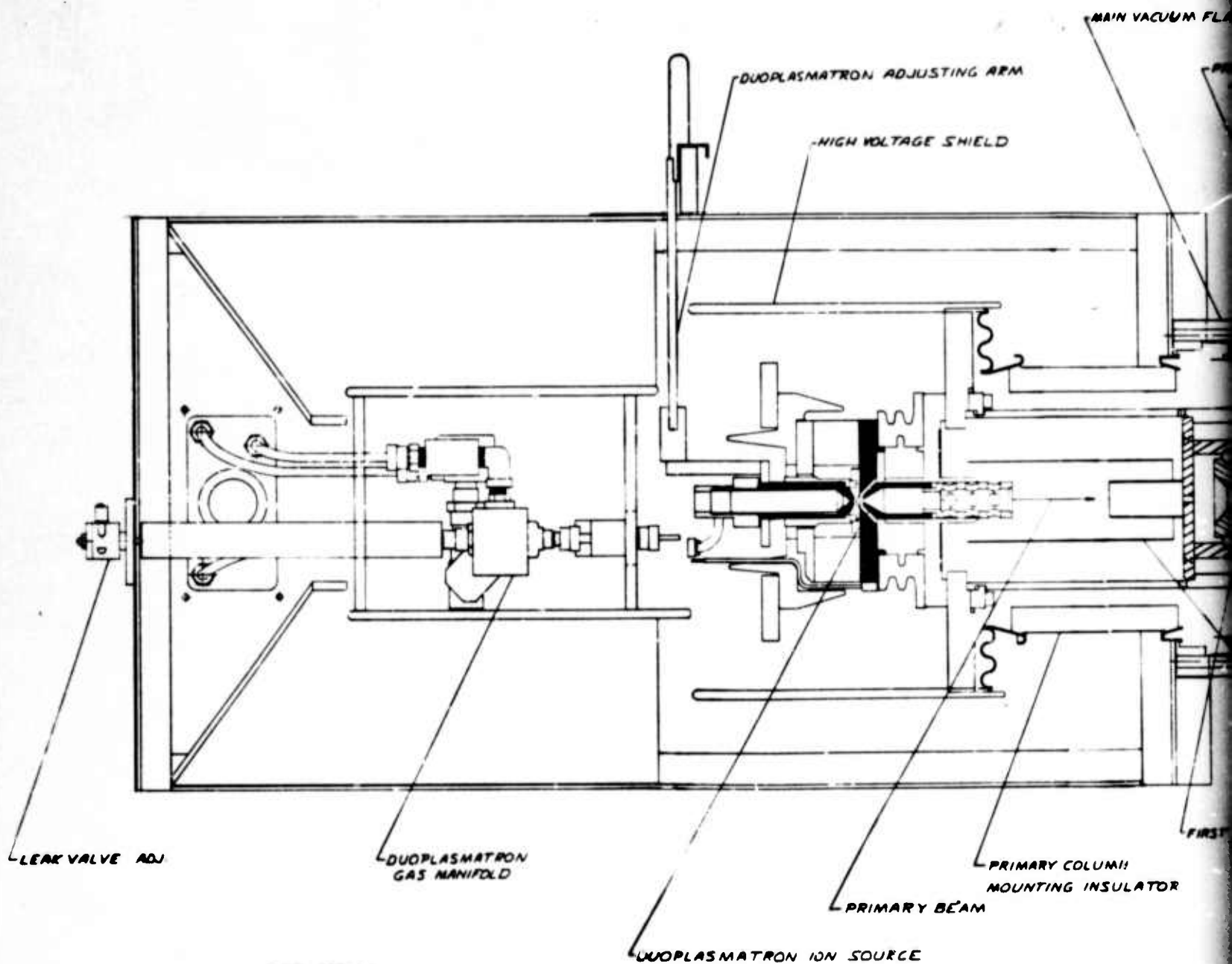
The Advanced Ion Microprobe (AIM) is basically an ion source unit for an analytical mass spectrometer. It generates ions from the atoms which make up the matrix of a solid sample and accelerates these ion in the proper direction and with the proper energy so the charge-to-mass ratio of the ions and

their abundance can be measured in the mass spectrometer. The resulting data permits the analyst to determine the chemical and/or isotopic composition of the sample.

The AIM creates ions from the surface of a sample by striking the sample with a very small diameter beam of very high velocity (20 kev) ions of selected gasses (oxygen, nitrogen, argon, etc). These impinging primary ions remove the atoms from the sample surface via a sputtering process which also ionizes a large portion of the sputtered sample atoms. The ionized sputtered atoms are then called secondary ions. See Figure 1 for an illustration of the major components of the AIM.

The sputtered secondary ions are prepared for analysis by the mass spectrometer by the secondary ion column. The secondary ion pickup electrode provides the initial extraction of the secondary ions from the vicinity of the sample and accelerates them to a moderate energy (1.5 kev) and into the immersion lens. The immersion lens further accelerates the ions up to the final energy (15 kev) required by the mass spectrometer and also focuses them through the secondary ion slit which acts as the object point for the mass resolving system.

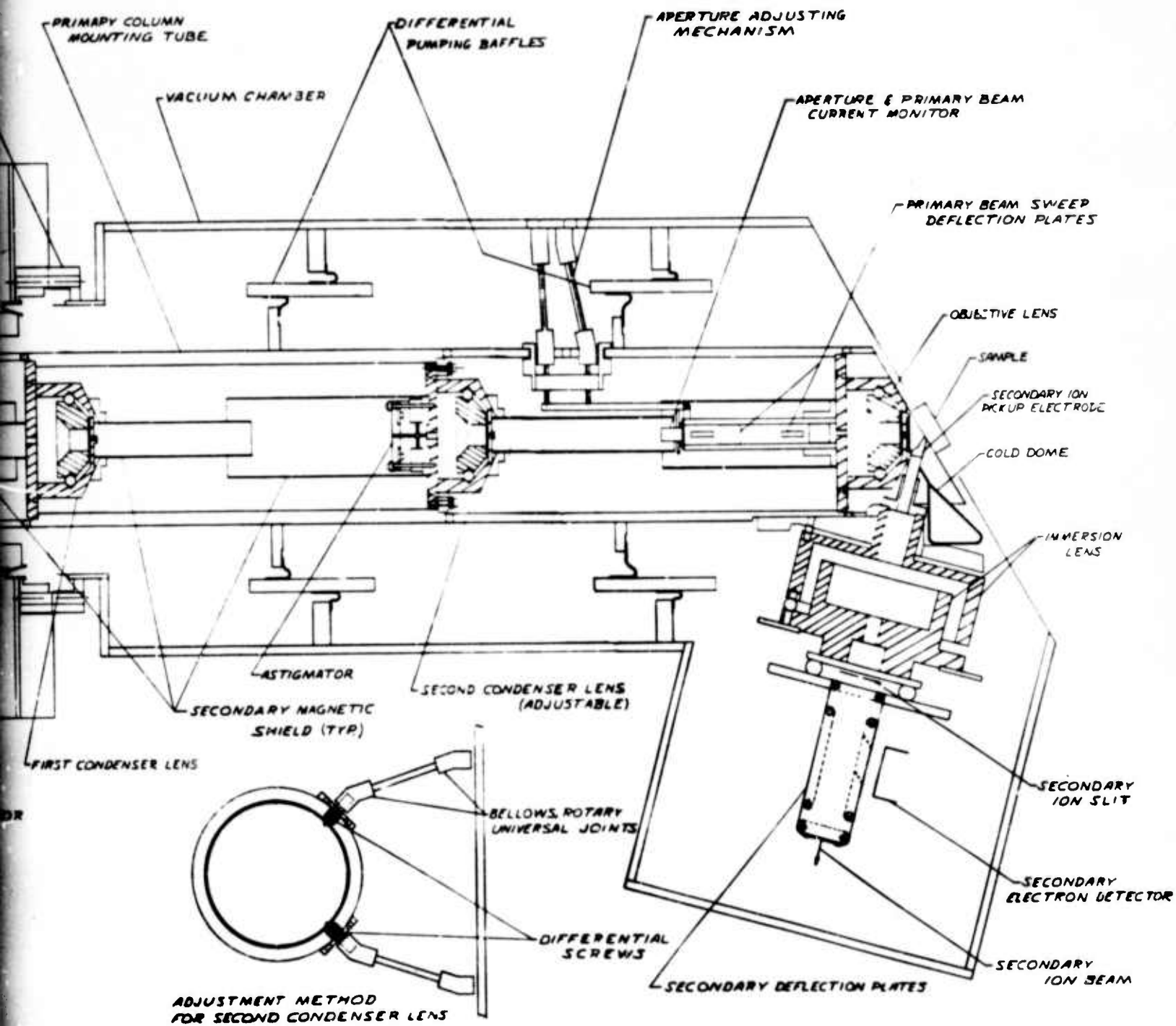
The primary ions striking the sample generate large quantities of secondary electrons as well as secondary ions. The secondary electrons can be used to image the topography of the sample in a manner similar to a scanning electron microscope. Since the system uses only electrostatic fields in its optics, the secondary electrons will be collected and focused in a manner similar to the secondary ions. This permits the secondary electron detector to be placed after the secondary ion slit.



TOP VIEW
 ADVANCED ION MICROPROBE
 FIGURE 1

A

VACUUM FLANGE



B

The primary ions are created by a plasma discharge in a partial vacuum of the selected gas in the duoplasmatron ion source. The selected gas is metered into the ion source by the gas manifold.

The beam of primary ions from the duoplasmatron ion source is focused into a very small diameter spot on the sample surface by the action of three electrostatic lenses, the first condenser lens, the second condenser lens and the objective lens, in the primary ion column. A set of electrostatic deflection plates just before the objective lens permits the primary ion beam to be moved across the sample surface. A primary beam current monitor located between the second condenser lens and the deflection plates permits the primary beam intensity to be continuously monitored. An electrostatic astigmator located just before the second condenser lens permits a reduction in astigmatism of the focused primary beam.

The critical focusing of the primary ion beam is protected from the degrading effect of external magnetic fields by the primary shielding effect of the iron primary column mounting tube and the secondary shielding effects of the iron lenses and the "mu-metal" secondary magnetic shielding tubes. The magnetic shielding for the secondary ion column is provided by the iron construction of the immersion lens and secondary electron detector deflection plates.

Proper functioning of the instrument requires that it operate in a very high vacuum. The vacuum is provided by a three-stage differentially pumped vacuum chamber which is isolated into three compartments by the differential pumping baffles. The differentially pumped system permits the high gas load from the duoplasmatron ion source to be efficiently pumped while maintaining extremely low pressures at the sample.

A liquid nitrogen cooled cold dome is provided which completely surrounds the sample surface in the analysis position. The cold dome acts as an efficient trap for any residual gas molecules which remain in the vacuum system and might condense on the sample surface.

4. DESIGN OF THE ADVANCED ION MICROPROBE

4A. DISCUSSION OF PHASE I

At the original conception of the project it was determined that acceptable levels of performance were unobtainable with existing "state-of-the-art" primary column objective lenses. The spherical aberration of the available lenses was sufficiently high that the attainment of acceptable spot sizes required very small apertures for the lenses which reduced the current densities delivered to the sample to unusable levels.

Before undertaking the actual construction of hardware it was obvious that the feasibility of a superior objective lens would have to be determined. Therefore, Phase I* of the development of the AIM was undertaken to utilize computerized ion ray tracing techniques to develop a lens design with sufficiently low spherical aberrations that meaningful analyses could be made in the desired range of spot sizes. The Phase I contract resulted in a new lens design which reduced the spherical aberration (C_3) from 198 cm for the commercial IMMA to a value of 39 cm. This theoretical lens design predicted a potential of 0.1 μ spot sizes with usable current densities. Based on the results of the Phase I study it was decided to proceed with Phase II of the project, the actual design and construction of an AIM system, which is the subject of this report and contract.

* Contract F33657-71-C-0523: "Feasibility Study of Altering the IMMA Source Generating System to Interface with the AFSEL/VIMS"

4B. RESULTS OF COMPUTER DESIGN

4B(1). Objective Lens

At the start of this contract, further computerized ray trace lens studies were made to give us a lens which would not only result in a low spherical aberration but would be physically realizable in terms of interfacing with the secondary ion column requirements, the cold dome, etc. This resulted in a configuration with an even better spherical aberration coefficient of 23 cm and a theoretical spot size limit of about 0.05 micron. The computer configuration is shown in Figure 2 and the actual mechanical configuration is shown in Figure 3.

The focal working distance versus excitation ratio is shown in Figure 4.

Using the information shown in Figure 5, which shows the spherical aberration effects for parallel rays of ions entering the lens at various distances from the axis, the effects of aperture centering were estimated.

<u>APERTURE DIAMETER (at lens)</u>	<u>DISTANCE OF APERTURE CENTER FROM LENS AXIS</u>	<u>ESTIMATED MINIMUM SPOT SIZE</u>	<u>ESTIMATED SIZE OF DISK OF CONFUSION IN PLANE OF FOCUS</u>
300 μ	centered	183 \AA	183 \AA (round)
300 μ	50 μ	433 \AA	200 x 503 \AA
400 μ	centered	433 \AA	433 \AA (round)
400 μ	25 μ	633 \AA	470 x 766 \AA
400 μ	50 μ	783 \AA	500 x 1033 \AA
400 μ	100 μ	1333 \AA	530 x 2000 \AA

These data are for an aperture located at the lens i.e. the aperture diameter would correspond to the diameter of a column of parallel ions entering the objective lens.

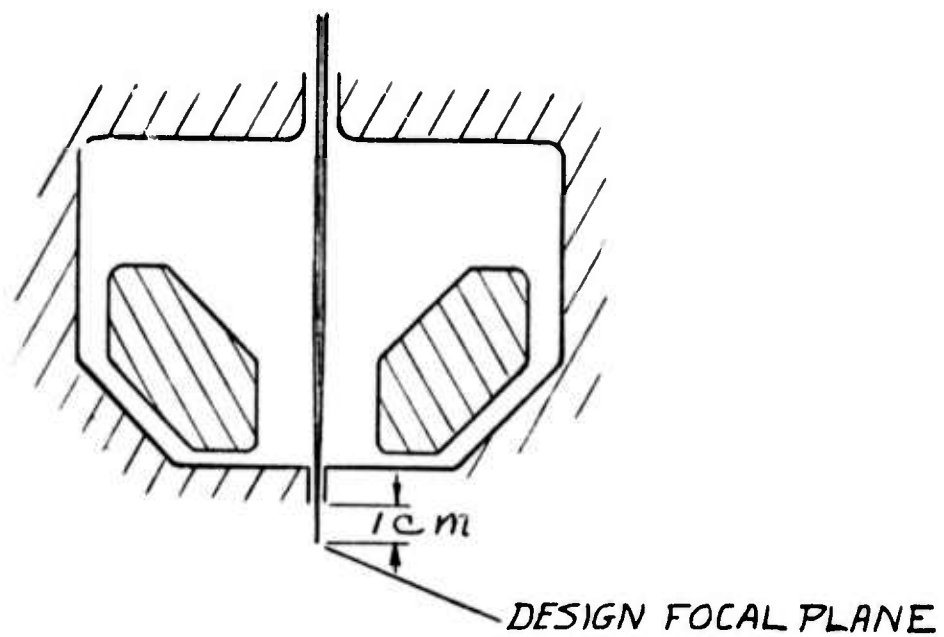


FIGURE 2: COMPUTER RESULTS OF OBJECTIVE LENS DESIGN

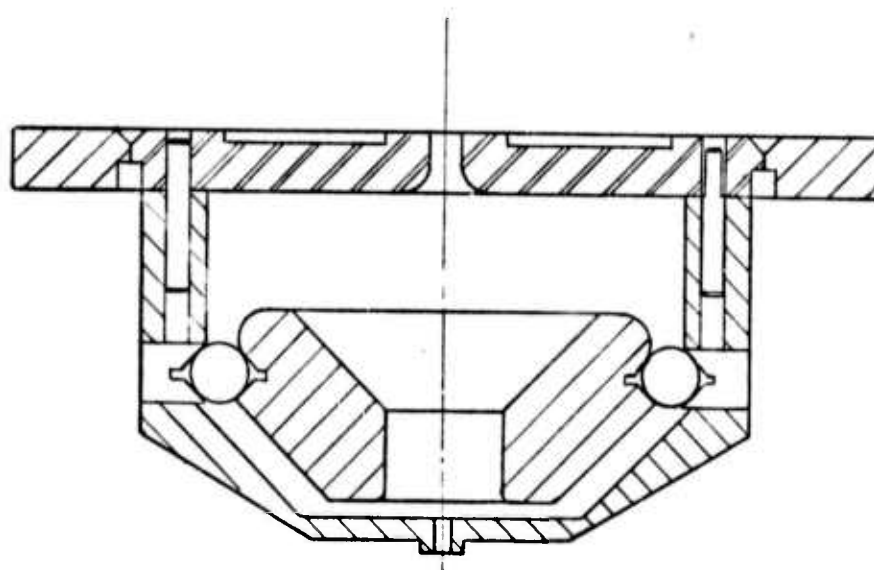


FIGURE 3: ACTUAL MECHANICAL DESIGN OF OBJECTIVE LENS

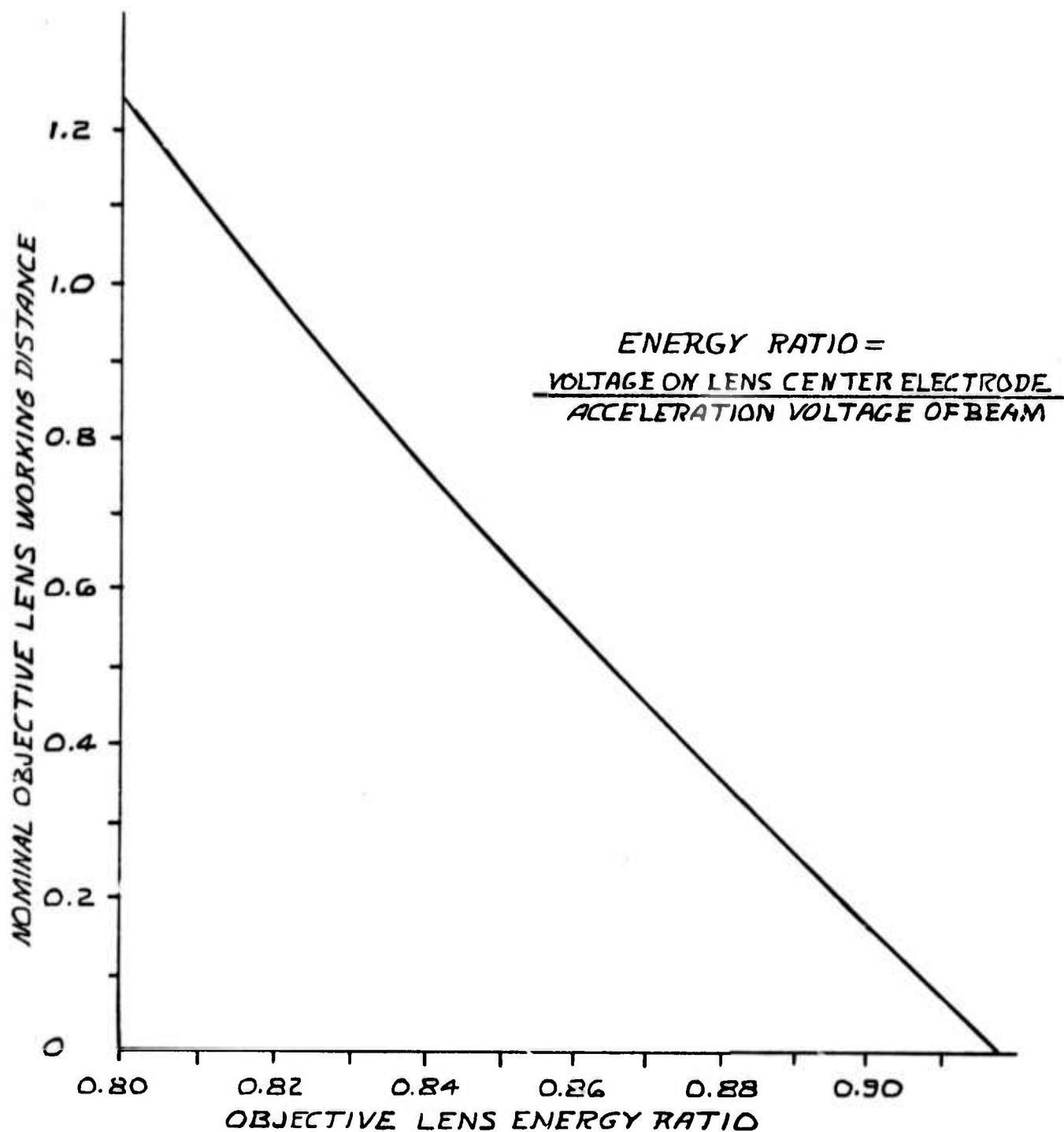
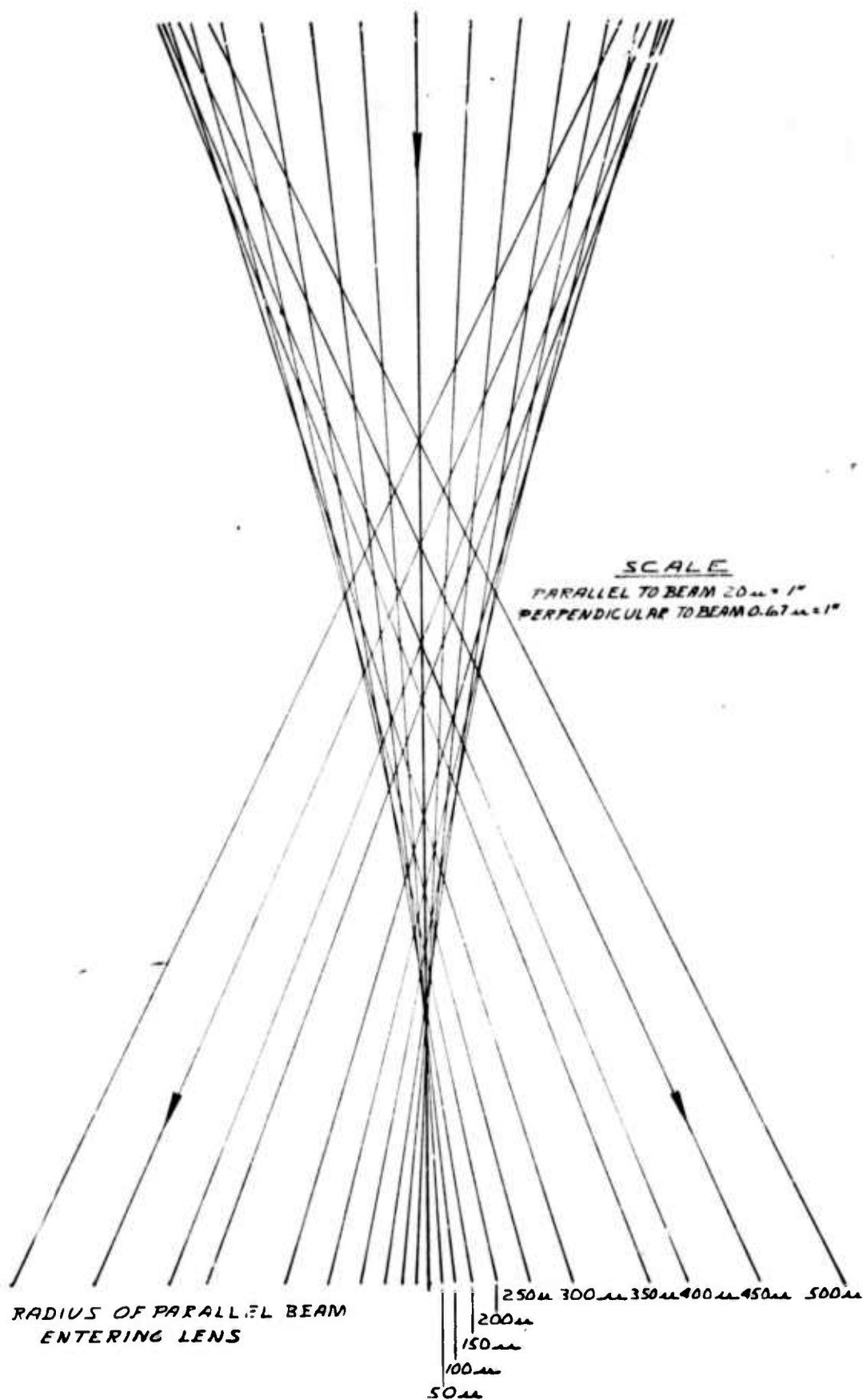


FIGURE 4: OBJECTIVE LENS NOMINAL WORKING DISTANCE VERSUS EXCITATION RATIO

FIGURE 5: OBJECTIVE LENS FOCUS SHOWING SPHERICAL ABERRATION



The data graphically shows the importance of centering the primary beam on the objective lens. The centering must be done to precisions of much better than 25 microns to avoid severe deterioration of performance.

4B(2). Pickup Electrode and Immersion Lens

The tilted sample configuration for the objective lens and pickup electrode was dictated by considerations of the optical viewing path, physical clearance for the pickup electrode relative to the objective lens, and the objective lens working distance. An ion optics benefit was derived from this purely mechanical design compromise. The computerized ion ray traces showed, and the tests later confirmed that an increase in transmitted secondary ion current was possible by operating the equipotential surface formed by the cold dome and objective lens at a potential somewhat higher (300 to 800 volts) than the pickup electrode potential. The tilted configuration of the cold dome relative to the sample enables this bias to repel the secondary ions towards the pickup electrode.

The virtual object formed by the secondary ions passing through the pickup electrode is very confused. (See Figures 6 and 7.) This poor quality object will limit the quality of the focus achievable at the secondary ion slit. When the polarity of the secondary beam relative to the primary beam is changed, the location of the virtual object will shift due to the lateral deflection of the primary beam after it leaves the objective lens. This deflection is caused by the attractive or repulsive force of the field from the pickup electrode. This shift in position as well as the nominal pickup electrode geometry is shown in Figure 8. The virtual object shifts approximately 0.15 mm laterally and 1.3 mm longitudinally relative to the axis of the secondary column. The nominal object point of the pickup electrode-immersion lens optics was placed approximately halfway between these two points.

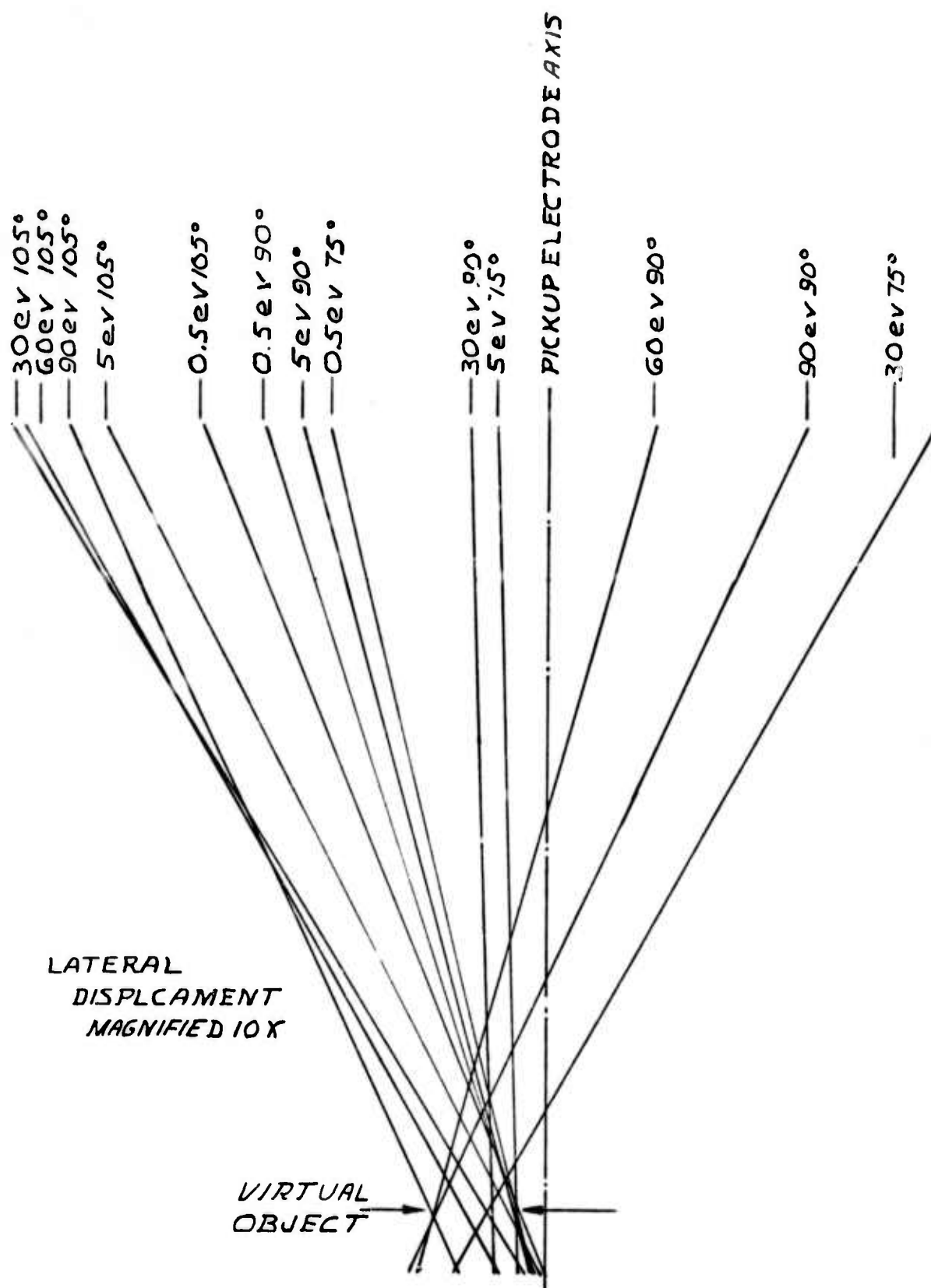


FIGURE 6: VIRTUAL OBJECT CREATED BY SECONDARY ION PICKUP ELECTRODE FOR SAME POLARITY PRIMARY AND SECONDARY IONS (30 VOLT BIAS ON COLD DOME)

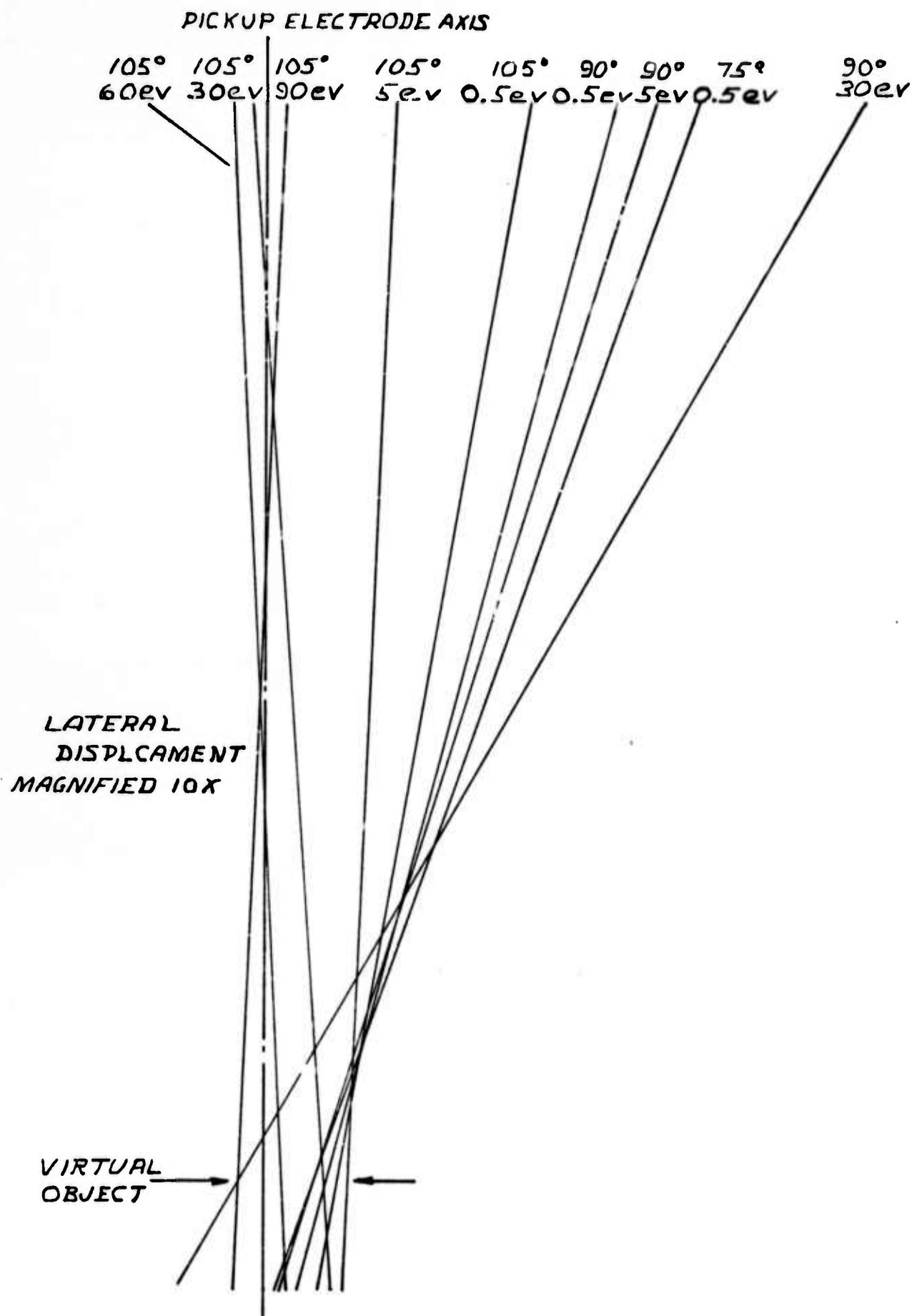


FIGURE 7: VIRTUAL OBJECT CREATED BY SECONDARY ION PICKUP ELECTRODE FOR OPPOSITE POLARITY AND SECONDARY IONS. (300 VOLT BIAS ON COLD DOME)

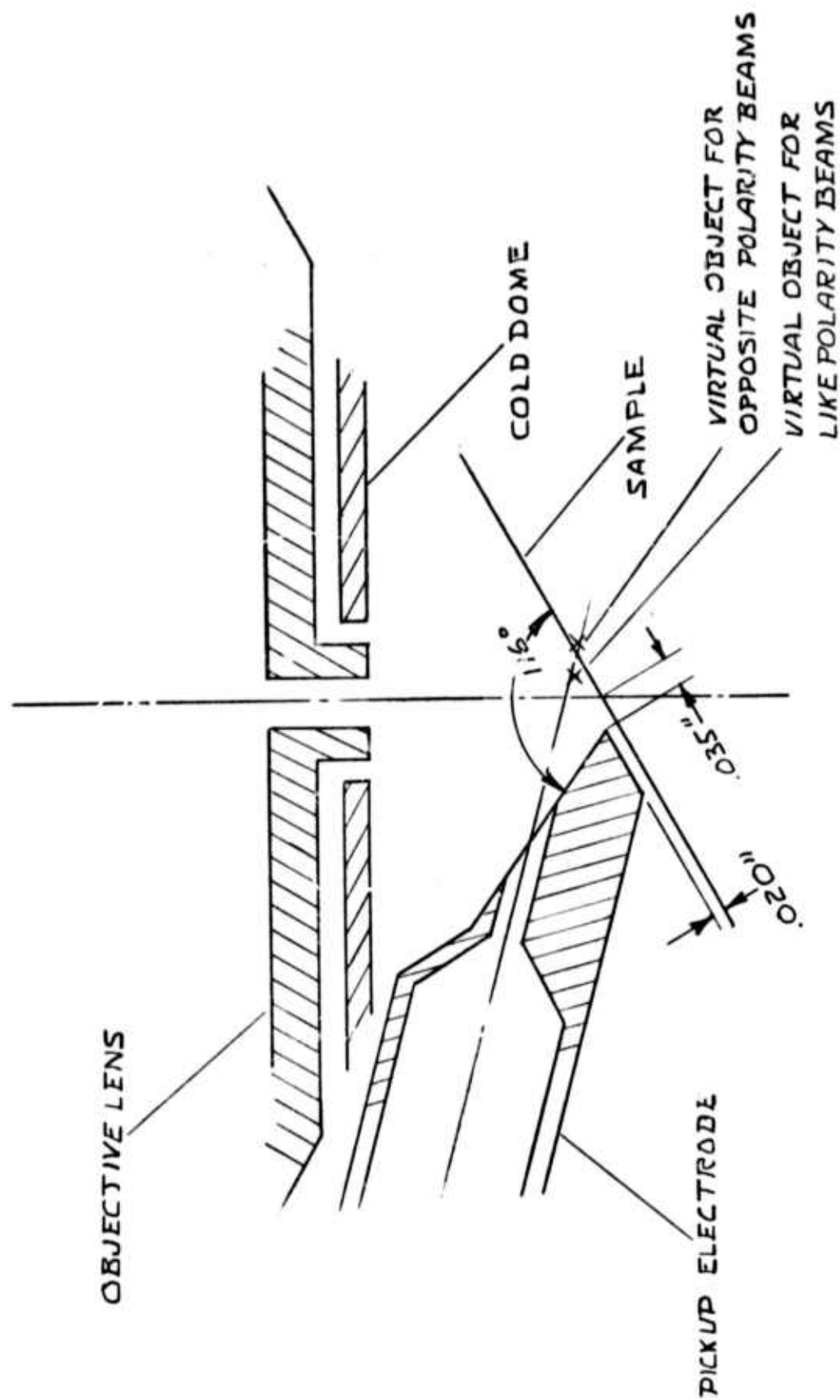


FIGURE 8: SECONDARY ION PICKUP ELECTRODE CONFIGURATION SHOWING VIRTUAL OBJECT LOCATION FOR DIFFERENT BEAM POLARITIES

The computer configuration of the immersion lens is shown in Figure 9. It is designed to have an object working distance of 6 cm and an image working distance of 2.82 cm. The lateral magnification is approximately 0.433 (i.e. image size = 0.433X (object size)) and due to the accelerating action of the lens, the angle of convergence of the ions approaching the image point is approximately 0.73 times the divergence angle of the ions leaving the object point.

4C. DETAIL DESIGN

4C(1). Selection of Basic Column Configuration

The combination of a 15 kev secondary beam and the low secondary ion extraction potential for the pickup electrode dictated the use of an immersion lens in the secondary ion column. The immersion lens transfers the secondary ions from the 13.5 kev potential of the pickup electrode down to the ground potential of the slit and the mass spectrometer and at the same time focuses the ions on the slit.

Two choices were available on primary column configuration. One had the source and condenser lenses at ground potential and used another immersion lens just before the objective lens to transfer the primary beam up to the 15 kev potential of the sample. The second choice eliminated the immersion lens in the primary column but required the source and the entire primary column to float at a potential close to that of the sample. The second approach was selected because, in part, it minimized aberrations, it enabled the duoplasmatron ion extractor electrode and the condenser lenses to work at a constant and optimum potential, and it reduced the size of the components. The disadvantages are that it requires the primary beam deflection plates and current monitor to float at high voltage and it would somewhat complicate the installation of a primary column magnet if one were desired at some future date.

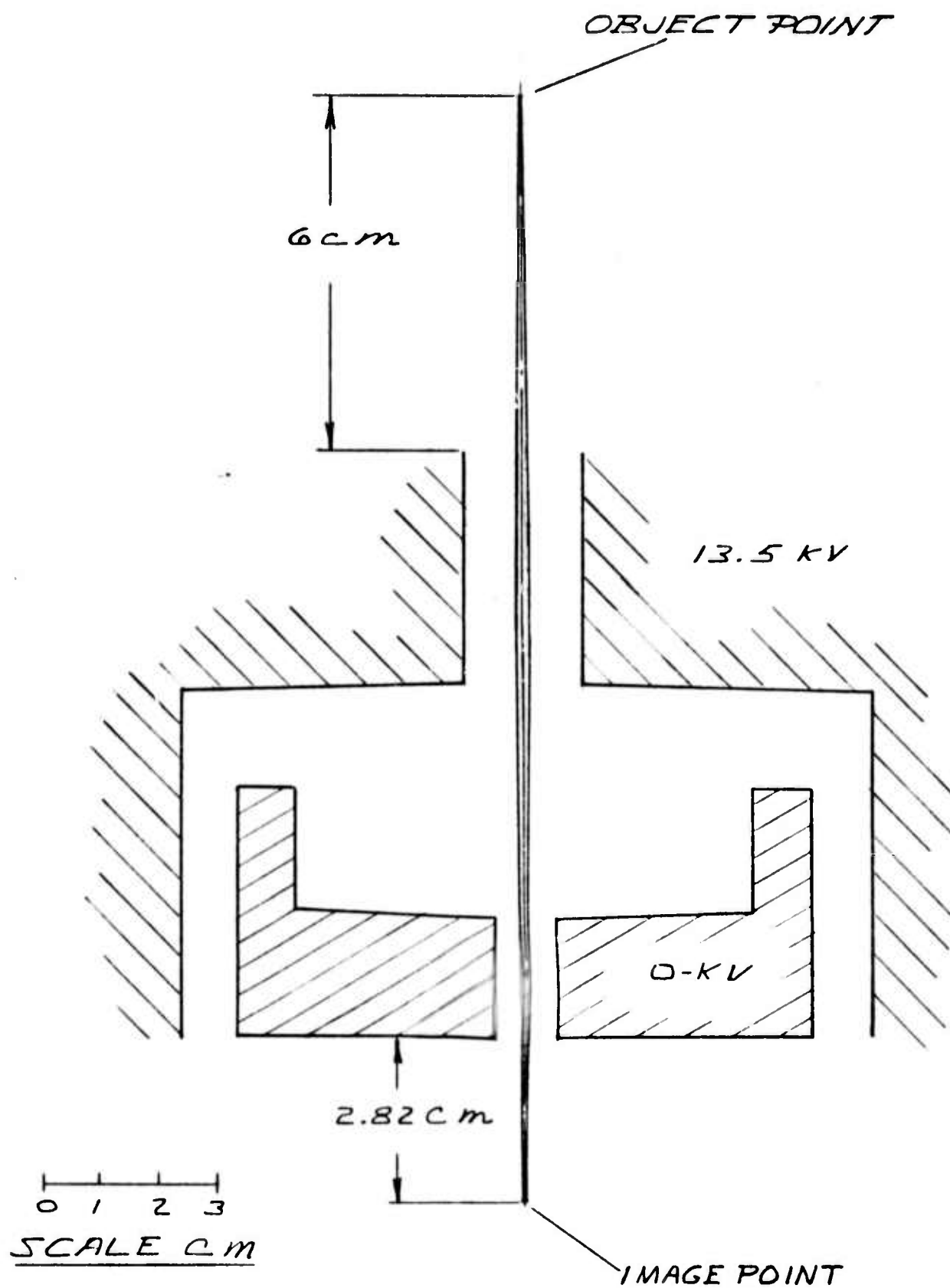


FIGURE 9: RESULT OF IMMERSION LENS DESIGN

A three lens primary column was selected to achieve the desired demagnification within a reasonable physical length.

It was desired to have the entire AIM system designed so it could be completely assembled on the bench and then installed through a single flanged opening on the vacuum system. Due primarily to the physical size of the immersion lens this would have required a very large, expensive, and difficult to use "Wheeler" type flange. It would have also greatly complicated the design and cost of the differential vacuum pumping system. As a result, it was decided to make the secondary ion column a prealigned module which could be easily plugged into the primary column after the primary column was installed in the vacuum chamber. This decision also greatly simplified the design of the secondary electron detector by allowing it to be located after the immersion lens.

4C(2). Primary Ion Source

The primary ion source is a slightly modified version of the standard ARL duoplasmatron with adjustable "Z" electrode as used on ARL's commercial Ion Microprobe Mass Analyzer (IMMA). The standard ARL source is well suited for generating 20 kev beams of positive or negative ions for this application. However, it is designed to function with its extractor electrode and mounting flange at ground potential rather than at the 13.5 to 14.5 kv of the floating primary ion column of the AIM.

The only modifications made to the duoplasmatron were to permit it to be floated at this higher potential. The modifications consisted of a longer dielectric handle on the "Z" electrode adjustment, a corona shield surrounding the source at the potential of its mounting flange, and a redesigned gas manifold capable of withstanding the 35 kv required for the floating duoplasmatron. The remainder of the source uses off-the-shelf ARL parts to permit convenient and economical repair and maintenance.

The relative abundance of positive or negative ions and electrons varies across the width of the plasma in the duoplasmatron. The positive ions and electrons are most abundant in the center and the negative ions are relatively more abundant towards the periphery of the plasma. The "Z" electrode determines the position of the plasma relative to the ion extraction hole in the anode. By moving the "Z" electrode relative to the anode, the yield of the desired charged particle can be optimized. The adjustable "Z" electrode is achieved by making the electrode in two parts with a nonconcentric interface and then rotating one part relative to the other.

The gas manifold is very similar to the one used in the ARL IMMA. The higher dielectric isolation required in the AIM was achieved by mounting the components in a cylindrical corona shield and isolating that by large air spacings and an acrylic support. The corona shield is designed with a series of holes in each end of the cylinder to provide for air flow in the event forced air cooling of the duoplasmatron is required in the future. This modification would require the addition of a fan and two plastic collars.

The gas manifold is designed to slide on its support away from the duoplasmatron to permit servicing of the source without disconnecting anything except the lines to the duoplasmatron and the flange which supports the leak valve adjustment mechanism.

The normally used needle type leak valve has been replaced with a much more stable and reproducible type of valve. It is basically a rotating ball valve with a 0.0005" groove in the periphery of the ball. The adjustment of the valve is made via an insulating shaft and a worm gear and dial on the outside of the high voltage enclosure.

The gas manifold is equipped to carry a standard thermocouple or thermopile vacuum gauge tube and it has a pneumatically actuated valve to permit rapid pumpdown of the source via a separate line.

The gas manifold corona shield contains a terminal block to connect the high voltage supply cable to the duoplasmatron leads. The resistors to provide "Z" electrode bias and cathode drop are mounted on this terminal block. The high voltage cable and the gas and vacuum lines are brought into the corona shield through the vent holes in the rear of the shield.

A major problem in the system design was achieving the required vacuum at the sample while pumping the gas load which leaks through the ion extraction hole in the duoplasmatron anode. This gas load is estimated at 2 to 3×10^{-4} torr·liters/second. The bulk of this gas load is pumped at a pressure in the mid 10^{-6} torr range in the first stage of the differential pumping system above the first condenser lens.

4C(3). Column Mechanical Mounting

The mounting structure for the ion optics elements of the AIM must satisfy four primary criteria. It must provide a rigid, vibration free, and precise mounting for the ion optic elements. It must provide sufficient high voltage isolation to permit the column to be floated to the sample potential. It must provide magnetic shielding. And, it must be vacuum compatible, providing for the differential pumping baffles while allowing adequate conductance for effective pumping in each stage.

The basic mechanical structure is the primary column mounting tube which consists of a five inch diameter cylinder machined from a single forged billet of Armco iron. This tube

contains three shoulders which locate the three primary column lenses on a common axis with a high degree of precision. In addition the center lens (second condenser lens) is provided with an external mechanical centering mechanism via differential screws and insulated shafts. This allows adjustment of the lens centering to compensate for the slight flexing of the tube under atmospheric pressure loading and for variations in machining tolerances. The upper end of the tube is located to the duoplasmatron mounting flange by a precision shoulder and is held by a set of clamps. The duoplasmatron is precisely located to this same flange by a dowel and diamond pin combination. Provision has been made for future installation of an adjustment mechanism at the base of the duoplasmatron which can be incorporated with only minor modification which will permit the duoplasmatron to be independently aligned to the system.

The secondary ion column is mounted on a flat machined on the side of the primary column tube at the sample end. The secondary column is located relative to the objective lens by a dowel pin and two diamond pins and is held by two screws permitting easy removal and installation while maintaining alignment.

The high voltage isolation and the mechanical support of the system is provided by two components. The upper end of the primary column is supported by a metal diaphragm which is attached to the outside of the duoplasmatron mounting flange. The inside edge of the diaphragm is connected to one end of the primary column mounting insulator. The other end of the insulator fastens to the main vacuum flange. This assembly rigidly locates the upper end of the tube in the lateral directions but permits some longitudinal freedom via the flexible diaphragm. The main vacuum flange is a rotary flange so no rotational constraint is provided at this end of the column until the flange is tightened. This support assembly is vacuum tight and acts as a continuation of the vacuum chamber.

The sample end of the primary column mounting tube is carried by two one-inch insulating ceramic balls. One ball seats in a round socket on the underside of the tube just toward the sample from the objective lens mounting shoulder. The second ball rides in a "Vee" groove parallel to the primary beam axis on the upper side of the tube. These balls are clamped into their sockets on the tube by an antivibration mounting yoke which is rigidly mounted to the same end plate of the vacuum system that carries the sample stage. This is done to minimize the vibration of the sample relative to the objective lens. The lower ball locates the height of the column at the sample and provides lateral and longitudinal location of the column in the horizontal plane. The upper ball provides rotational constraint of the column about the primary beam axis.

The primary magnetic shielding for the primary ion column is provided by the annealed and degaussed Armco iron construction of the primary column mounting tube. A secondary magnetic shield is provided by pairs of telescoping "Mu-Metal" tubes in the drift space between the lenses and between the duoplasmatron and the first condenser lens. The primary column lenses are also made of annealed Armco iron and are magnetically insulated from the primary column mounting tube so the lens housings act as a secondary magnetic shield and their center electrodes act as a tertiary magnetic shield in the region of highest magnetic field sensitivity of the ion beam. The shielding factor is low at the sample surface, being approximately a factor of three due to the end of the column tube being flush with the sample surface. The shielding factor at the sample will be supplemented greatly through the use of a high magnetic permeability sample holder on the stage. The next lowest shielding factor is in the duoplasmatron ion extractor where the shielding factor is approximately 30. At the upper entrance to the column tube the factor becomes 300 and increases rapidly to over 3000 for the rest of

the primary ion trajectory except for the interior of the lenses where the factor drops to 200 to 300.

The magnetic shielding of the secondary ion column is provided by the annealed Armco iron construction of the immersion lens and secondary electron detector deflection plates and by a rolled tube of "Mu-Metal" inside the secondary ion pickup electrode tube.

The three chambers for the differentially pumped vacuum system are obtained by compartmenting the outside of the primary column mounting tube by two flanges welded to the tube which press against thin kovar disks on the insulating differential pumping baffles. The baffles, in turn, mount on walls of the vacuum chamber completing the compartment. The chamber with the highest vacuum consists of the entire secondary ion column and sample region. The intermediate vacuum chamber consists of the interior of the primary column mounting tube between the first condenser lens and the objective lens and the region outside the tube between the two differential pumping baffles. The gas load from this region of the tube is pumped through a series of one inch holes in the sides of the tube between the two baffles. The highest pressure region occurs between the duoplasmatron and the first condenser lens. The bulk of the gas load from the duoplasmatron is pumped through another set of one inch holes in the sides of the tube between the duoplasmatron mounting flange and the first condenser lens. To ensure compatibility with the high vacuum, all parts subject to corrosion have been electroless nickle plated with some components receiving additional gold plating.

4C(4). Primary Column Lenses

To simplify and economize design and fabrication, the same basic lens design is used for all three primary column

lenses. However, due to the extremely tight hand fit tolerances required for acceptable aberrations, the individual parts of the lenses are not interchangeable. In addition, each lens has been hand fitted to its own mounting shoulder in the primary column mounting tube to ensure concentricity. A spare lens has been provided which has two sets of cover plates which permit it to be used in any of the three locations.

The computerized lens studies showed that asymmetrical lenses reduce aberrations; however, the degree of asymmetry is limited by high voltage breakdown of the elements. A voltage gradient of 100,000 V/cm was used as a practical upper limit in the lens design.

The acute space problems associated with the magnetic shielding, the pickup electrode and the differential pumping baffles led to the use of a ball bearing style construction for the lenses. The final machining of the inner surfaces of the lens was done with the lens assembled to ensure intrinsic concentricity of the elements.

The lens cup, the center element, and the lens cover are made from annealed Armco iron which has been electroless nickel plated and then gold plated to ensure good surface electrical conductivity and freedom from corrosion. The outer rim of the lens cover where it seats into the shoulder of the primary column mounting tube is stainless steel which has been welded to the center iron section. The stainless steel provides the magnetic insulation for the secondary magnetic shield as well as a more durable surface for the removal and reinsertion of the lens. The stainless steel has been treated with "Microseal" dry film lubricant to protect against galling. The lens cup has six holes around its periphery to provide for vacuum pumping, insertion of the ceramic insulating balls which

carry the center electrode, and for the high voltage terminal for the center electrode.

The differential screw lateral adjustment mechanism for the second condenser lens provides a motion of approximately 0.010 inch per revolution and is driven from outside the vacuum system by insulating ceramic rods and bellows type universal joints.

4C(5). Primary Ion Beam Deflection System

The primary ion beam deflection system is used to move the focused primary ion beam over the surface of the sample. This is done with two pairs of electrostatic deflection plates for each axis of deflection. The deflection plates are located just before the objective lens. The use of two pairs of deflection plates permits the beam to be "pivoted" about the nominal center of the objective lens thereby minimizing the aberrations of the beam as it is being deflected. If the beam is allowed to go through the lens off center the aberrations are severely increased as discussed in Section 4B(1). The pairs of deflection plates are made with large aspect ratios of length and width to separation to minimize the distortion of the beam due to fringing fields at the edges of the plates.

The deflection plates are mounted in an electron discharge machined aluminum frame which mounts directly on the objective lens cover. The individual deflection plates are made of aluminum and are heavily anodized in selected areas to insulate them from the mounting frame. The portion of the plates exposed to the ion beam are gold plated. Each plate is equipped with a sealed spark gap unit connected to the frame to protect the anodized insulation from high voltage transients.

4C(6). Primary Beam Aperture

The limiting aperture for the primary ion column optics is located at the end of the deflection plate frame away from the objective lens. This location, before the deflection plates, is forced by the type of deflection system and the nature of the electrostatic lens. In general, it is not desirable to have the aperture this far away from the objective lens because of the small diameter aperture which is required. However, the advantages of the double deflection plate system plus the ability to optimize the effective angular aperture for desired spot size by manipulation of the relative demagnification of the two condenser lenses hopefully offsets any disadvantages of the small size aperture.

The combination of the aperture location plus the use of two condenser lenses permits the effective angular aperture at the objective lens to be adjusted independently of the total column demagnification. This, in turn, permits the objective lens angular aperture to be optimized to give maximum current in the selected size spot. For an objective lens with spherical aberration coefficient, C_s , the maximum current density in a spot of diameter d is achieved if:

$$J = C_s \alpha^3$$

where α is the half angle of the cone of ions converging onto the sample. By adjusting the demagnification of the objective lens so its object point is the proper distance before the aperture, the desired α can be obtained. Since there are two independent condenser lenses, the crossover point (or focus) of the second condenser lens can be placed at the object point required by the objective lens for the correct value of α and at the same time the total system demagnification required to produce a spot size " d " can be obtained. This is virtually equivalent to having a mechanically adjustable aperture at the objective lens.

The alignment requirements of the aperture (See Section 4B(1).) are critical for proper performance of the AIM. This necessitates an externally adjustable aperture. The adjustment is obtained by a pair of rotary vacuum feedthroughs driving a pair of screw shafts mounted on the primary column tube via insulated coupling rods. The screw shafts actuate a pair of class two levers whose fulcrum is on the aperture end of the primary deflection plate frame. The levers move a hardened stainless steel plate carried on the end of the deflection plate frame by a ball thrust bearing and springs. The hardened stainless steel plate carries the aperture and the primary beam current monitor. The overall system allows for extremely fine motion of the aperture (50 to 70 microns/revolution).

The optimum size of the aperture is 75 to 100 microns and standard catalog electron microscope apertures are used.

4C(7). Primary Beam Current Monitor

The primary beam current monitor is constructed as an integral part of the primary aperture system. It is designed so it gives a continuous signal which can be monitored simultaneously with the analysis of the sample.

The monitor consists of a long thin metal tube supported by a sapphire insulator which has the end of the tube away from the primary ion source partially blocked by the primary beam aperture. This closed end tube acts as an excellent faraday cup for capturing the ion (or electron) beam entering the open end of the tube without losing significant charge due to secondary electrons. The small hole at the bottom end of the tube (the aperture) permits a small fraction of the intercepted beam to pass on through the faraday cup to the objective lens and sample. Immediately preceding the faraday cup tube is another aperture which is electrically "grounded"

to the primary column mounting tube and is about six times larger in diameter than the primary beam limiting aperture. This larger aperture is much smaller than the entrance to the faraday cup tube so it performs two functions. It ensures that the beam which enters the cup strikes the internal surfaces of the cup well down inside the tube. This ensures retention of the secondary electrons. It also provides a well defined diameter to the beam entering the cup so the fraction of beam exiting the cup through the limiting aperture will be a constant fraction of the signal collected by the cup. As a result, for a fixed demagnification in the primary column, the current monitor signal will always maintain a constant proportionality to the beam current delivered to the sample. Typically, the monitor current is 30 to 40 times the sample current.

The current collected by the faraday cup is fed into a shielded cable through a spring wire "cat's whisker" which contacts the side of the faraday cup tube.

4C(8). Astigmator

An eight pole electrostatic astigmator is mounted on the cover of the second condenser lens. Although the need for this unit has not yet been experimentally demonstrated, it has been installed as an aid to improving performance in the future.

4C(9). Visual Optics

An optical path for viewing the sample surface during analysis has been provided which will permit the use of an optical microscope with a working distance of 1.8" or greater. The viewing path passes over the edge of the sample and reflects off of a mirror mounted on the bottom of the objective lens just below the pickup electrode. The angle of incidence of the viewing path is tilted 31 degrees from a perpendicular to the sample surface.

4C(10). Cold Dome

The liquid nitrogen cooled cold dome is mounted on the sample side of the objective lens. It is shaped so the chilled metal surface subtends a full 2π solid angle from the sample surface except for the openings for the nose of the objective lens, the viewing optics mirror, and the secondary ion pickup electrode. The cold dome is constructed with a liquid nitrogen reservoir of approximately 40 cc capacity. It has a stainless steel bellows liquid nitrogen feedline coming into the bottom of the reservoir and an identical bellows for a vent coming out of the top of the reservoir. By connecting a dewar to the lower feedline external to the vacuum system and maintaining the level of nitrogen in the dewar at a height equal to midpoint of the cold dome reservoir, the liquid will seek its own level and a supply of liquid will be maintained in the cold dome with a minimum of vibration and percolation.

The body of the reservoir and the metal surface between the objective lens and sample are made from a single sheet of OFHC copper to ensure optimum thermal conductivity. The cold dome is rigidly supported and thermally insulated by six very thin stainless steel strips which connect to the base of the objective lens and to the primary column mounting tube.

Since the cold dome and objective lens are electrically connected, the cold dome acts as a continuation of the equipotential surface of the nose of the objective lens. This equipotential surface along with the pickup electrode and the sample surface determines the ion optics of the pickup electrode system.

4C(11). Secondary Ion Pickup Electrode and Immersion Lens

The secondary ion pickup electrode and the immersion lens are the basic components of the secondary ion column.

They are mounted as an assembly on a precision 15 degree stainless steel wedge. The wedge is then mounted on the side of the primary column mounting tube. The alignment of the secondary column to the objective lens and sample is very important. The secondary column components and wedge have been machined as a prealigned assembly which was then aligned to the objective lens and located with a precision dowel pin and two diamond pins. The use of the pins permits the secondary column to be removed and replaced on the primary column without disrupting the alignment. Minor fine alignment of the pickup electrode to the sample and objective lens is possible through the use of adjusting screws in the pickup electrode mounting flange located at the input to the immersion lens.

The first half of the immersion lens and the pickup electrode operate at 13.5 kv and are insulated from the wedge and primary column by four ceramic balls. The second half of the immersion lens is electrically grounded and is insulated from the first half of the immersion lens by four ceramic balls. The entire assembly is clamped to the wedge with tension screws and ceramic spacer insulators. The lens is made of annealed Armco iron for magnetic shielding and it has been electroless nickel and gold plated to protect against corrosion and ensure good surface conductivity.

4C(12). Secondary Ion Slit

The immersion lens focuses the secondary ions sputtered from the sample into a real image immediately after the lens. This real image is used as the object for the mass spectrometer optics. Since the virtual object created by the pickup electrode is poorly defined the quality of the focused real image may not be sharp enough for high quality mass analysis. This problem is solved by placing a slit at the position of the focused secondary beam which cuts off the fuzzy edges giving a sharp well defined object for the mass spectrometer optics.

To enable the operator to select the best tradeoff of signal level versus mass spectra quality an adjustable slit mechanism has been provided. The adjustable slit consists of a thin sheet of stainless steel with a series of four holes which act as the slit openings. This is mounted on a precision linear motion ball slide which can be moved via a feedthrough on the vacuum chamber. Each of the holes is a different size which enables the operator to select the best of the four slit openings for his particular problem.

For reasons associated with the ion optics of the mass spectrometer, it is desirable to have the length (or height) of the slit equal to one-half of its width. For this case, the slit openings are a set of rectangular holes whose dimensions are 0.005" x 0.003", 0.010" x 0.005", 0.020" x 0.010", and one very large opening which allows the full beam to pass. Since the small dimension is in the vertical direction, the vertical alignment of the slit is the most critical and the externally adjustable slit motion is in the vertical direction.

For cases where the restricted height of the slit is not necessary, a second slit assembly is available which has a more conventional long vertical slot for openings. In this case, the system is designed to have the slit motion in the more critical horizontal direction.

The slit assembly and ball slide are mounted on a plate which is fastened to the grounded exit portion of the immersion lens with two screws and is located with dowel pins.

4C(13). Secondary Electron Detector

The secondary electrons created at the sample are collected by the pickup electrode and are focused and accelerated by the immersion lens in a manner similar to the negative ions.

The detector for the secondary electrons works by deflecting the beam of electrons into a scintillator, light pipe, and photomultiplier tube assembly after they have passed the secondary ion slit assembly. When detecting electrons with a scintillator, it is desirable to have an electron energy greater than the 15 kev they have upon leaving the immersion lens. For this reason, additional acceleration is given to the electrons after they leave the immersion lens on the way to the scintillator.

The secondary electron detector deflection plates are located immediately after the grounded secondary ion slit assembly. The deflection plates are mounted in a rectangular four sided box which has a hole at one end for the ions and electrons to enter and a rectangular aperture at the exit end to limit the angular spread of the secondary beam as it enters the mass spectrometer when the secondary electron detector is not being used. When the electron detector is not in use, this entire assembly is electrically grounded; although, small voltage biases can be used on the plates to steer the secondary ion beam in a horizontal direction as it enters the mass spectrometer.

When secondary electrons are to be detected, the deflection plate to the right of the ion beam travel is grounded and the scintillator and the plate to the left of the beam are raised to a high positive voltage (+15 to 30 kev). The box which supports the plates is raised to one-half the voltage of the scintillator via a resistive voltage divider between the plates. When the electrons and negative ions leave the immersion lens-slit assembly they get accelerated as they pass into the box. Upon entering the box they see two plates of apparently equal voltage but opposite polarities and they are attracted to the positive polarity (left hand) plate.

The charged particles then pass through a hole in this plate and into the scintillator which is located immediately behind the hole. Since the deflection is electrostatic, the negative ions and electrons follow the same trajectory. The scintillator is covered with an opaque coating of aluminum to prevent charge buildup. The coating is thick enough to effectively stop the ions before they reach the scintillator but let the electrons pass.

The deflection plate assembly is made from annealed Armco iron for magnetic shielding and has been electroless nickel and gold plated. It is mounted to the secondary ion slit mounting plate with screws and ceramic balls.

5. TESTING AND RESULTS

The AIM was tested using the vacuum chamber, pumping system and electronics constructed by Vallecitos Nuclear Center (VNC) for use within the overall system when the AIM is installed on the Advanced Mass Spectrometer. This was done to avoid expensive duplications of equipment and to permit "shakedown" testing of the vacuum and electronics equipment at the earliest possible date.

A four-month period of extensive testing was scheduled but the bulk of this time was spent on troubleshooting and repair of electronics problems. Out of the four-month testing period, a total of only 21 days was spent in actual operation of the ion column.

5A. VACUUM SYSTEM

The VNC vacuum system consisted of the stainless steel vacuum chamber, two Varian two-cell ion pumps, two sorption type roughing pumps and manifold, a "Gasp" roughing pump, and a thermocouple gauge for measuring the pressure in the

duoplasmatron gas manifold. No sample stage or sample introduction valve was provided. We added an Aerovac residual gas analyzer (RGA) to accurately measure the vacuum pressures in the chamber.

After several months the empty "blanked off" chamber pumped to 2×10^{-8} torr. The RGA spectrum showed definite signs of carbon indicating the the original vendor did a less than satisfactory job of cleaning the chamber.

With the complete AIM installed in the vacuum chamber including a very crude sample holder, it would pump to 3×10^{-8} torr in several days time and the RGA spectrum indicated no increase in the "dirty" components of the residual gas. This clearly indicates that the AIM materials and cleaning methods were satisfactory.

The system was not tested with the differential pumping baffles installed for two reasons. The full set of vacuum pumps were not provided and the differential pumping baffles required modification to properly fit into the system. We performed the modifications to the baffles for VNC, but they were completed at too late a date for installation.

With the duoplasmatron in operation the system pressure was typically in the mid 10^{-7} torr range with both pumps operating.

5B. MECHANICAL

The mechanical assembly, alignment, and installation went very smoothly without any major difficulties. Only several problems are worthy of note. The previously mentioned differential pumping baffle problem involved a vendor dimensional error which we were able to correct. The antivibration yoke, which

mounts the lower end of the primary column, required modification and a number of locations on the vacuum chamber flanges required the installation of threaded inserts in place of nuts and bolts to permit accessibility for servicing.

The mechanical alignment adjustments work very smoothly with the exception of the second condenser adjustment which is subject to a small amount of "slip-stick" motion due to a sliding surface which was roughened more than desired during vacuum lubrication. Also the bellows used for universal joints for this lens adjustment are more flexible than desired resulting in some torque windup during adjustment.

5C. ELECTRONICS

The electronics provided by VNC consisted of a high voltage power supply for the primary column, a high voltage power supply for the secondary column, five high voltage resistive dividers to provide the various voltages required by the primary and secondary lenses, etc, an electrometer for the primary beam current monitor, a sweep system for the primary beam deflection plates, cables to connect to the vacuum feed-throughs, and a complete set of electronics for the secondary electron detector. We used our own duoplasmatron arc power supply since the VNC unit was not prepared for floating at high voltage. The typical operating voltages for the system are shown in Table I and figure 10.

5C(1). High Voltage Testing

Appropriate high voltage cables were made up to interconnect the various bridges, power supplies, etc. Since the special cables supplied for the primary beam deflection plates and current monitor were not capable of operating at high voltage, these elements were shorted to the primary column mounting tube whenever it was required to float the tube to high voltage such as for secondary column tests.

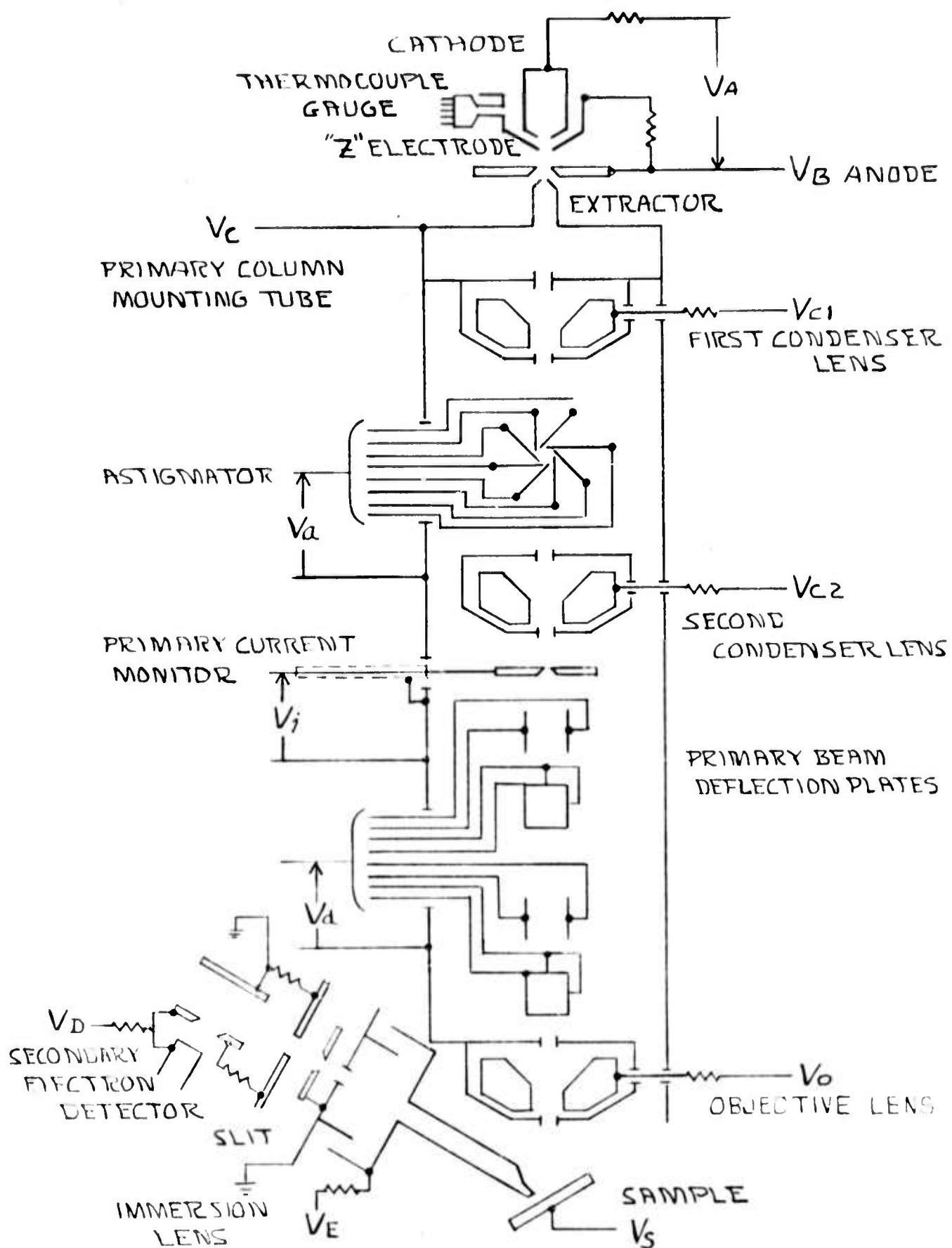


FIGURE 10: VOLTAGE SCHEMATIC

TABLE

TYPICAL OPERATING VOLTAGES (REFERENCE FIGURE 10)

		<u>+PRIMARY</u>	<u>-PRIMARY</u>	<u>+PRIMARY</u>	<u>-PRIMARY</u>
		<u>-SECONDARY</u>	<u>-SECONDARY</u>	<u>-SECONDARY</u>	<u>-SECONDARY</u>
V_A	Duoplasmatron anode relative to cathode		----- +500 to +600 V -----		
V_B	Duoplasmatron anode	+35 kV	-35 kV	+5 kV	- 5 kV
V_C	Primary column mounting tube and extractor	+13.5 to 14.5 kV	-13.5 to 14.5 kV	-13.5 to 14.5 kV	+13.5 to 14.5 kV
V_{C1}, V_{C2}	Condenser lenses	+25 to 33 kV	-25 to 33 kV	-5 to +3 kV	+5 to -3 kV
V_O	Objective lens	+31 to 33 kV	-31 to 33 kV	+1 to +3 kV	-1 to -3 kV
V_S	Sample	+15 kV	-15 kV	-15 kV	+15 kV
V_E	Immersion lens and secondary ion pickup electrode	+13.5 kV	-13.5 kV	-13.5 kV	+13.5 kV
V_D	Secondary electron detector and left deflection plate	grounded	grounded or +13 to 20 kV		grounded
V_d	Primary beam deflection plates relative to primary column mounting tube (V_C)		----- ± 100 V -----		
V_a	Astigmator relative to primary column mounting tube (V_C)		----- ± 100 V (estimated) -----		
V_i	Primary beam current monitor relative to primary column		~1 volt--dependent on electrometer input impedance		

NOTE: All voltages relative to ground except where noted

During all the testing and operation only one problem was found with the column associated with high voltage. On the last day of operation we experienced electrical breakdown between the two halves of the immersion lens. Upon disassembly, it was found that undersize insulating balls had been used in the previous assembly. This was corrected and no further problem is anticipated since this unit had earlier received extensive high voltage testing with the correct size insulators without failure of any kind.

Considerable high voltage difficulty was encountered with the electronics. A number of failures occurred in the divider bridges due to a variety of problems. A series of failures occurred in the sweep electronics as a result of high voltage transients (sparks) elsewhere in the system. The primary column power supply failed and had to be replaced with another unregulated unit whose specifications were not adequate for ultimate performance of the unit. The secondary column power supply failed several times and was given makeshift repairs. The thermocouple vacuum gauge for the duoplasmatron failed due to an arc requiring the last of the tests to be done based on the reproducibility of the leak valve setting.

5C(2). Primary Beam Sweep System

The inability of the cables for the primary beam deflection plates and current monitor to operate at high voltage made it impossible to use these functional features when the secondary column was being used. This made it impossible to use the superior secondary electron imaging technique for primary beam spot size evaluation and also made it impossible to get accurate estimates of the primary beam current incident on the sample during measurements of the secondary ion column efficiency.

The deflection plate drive electronics provided a "stair-step" sweep output. Each step represented a beam

deflection of greater than one-half micron so the system was not usable for evaluation of primary spot sizes less than several microns in diameter. As a result, a sweep system had to be jury-rigged to permit the beam to be swept in finer increments. Considerable time was spent devising a temporary system which would operate with equal voltages and opposite polarities referenced to ground and still have reasonably low ripple.

Just before the acceptance tests one of the deflection plates was found to be shorted to the primary column tube. Time did not permit the system to be disassembled to diagnose the cause of the short before shipment. It is probable that the short occurred as a side effect of an arc in the electronics that occurred during testing of the secondary column that also took out both sweep drivers, the vacuum gauge, and the secondary column power supply.

5D. ION TESTING

5D(1). Primary Beam Deflection and Current Monitor

The primary beam sweep system showed capabilities well in excess of specifications with deflections of up to 600 microns. The current to the sample was uniform over the specified sweep area to better than 10% with 5% being more typical.

Time limitations did not permit determining the optimum deflection plate voltage ratios which would give the beam crossover in the lens with the lowest aberrations although variations in performance could be noted with different ratios. Our best results were obtained for a nominal pivot point 2.8 cm above the sample surface.

The primary beam current monitor worked without flaw giving a strong and stable signal even during alignment of the aperture. The ratio of monitor current to sample current was on the order of forty to one.

5D(2). Primary Beam Spot Size

Due to the inability to use the secondary electron detector while scanning and due to the lack of a movable stage it was necessary to measure the primary beam size by scanning the beam over a fine metal mesh in the sample position while monitoring the current which passes through the mesh with a faraday cup behind the sample. The spot size measurements were limited by a variety of factors. The irregularities in the mesh were on the order of 0.1 to 0.2 microns. Ripple on the deflection plates was sufficient to cause appreciable blowup of the spot. And, the substitute primary column power supply had sufficient ripple to cause some spot size deterioration.

Typical observed performance was a spot diameter of 0.34 micron diameter with astigmatism less than 30%, and a delivered current of 2×10^{-11} amperes of positive air ions for a current density of 22 ma/cm². With identical focal conditions, a spot size of 0.55 microns with -3.5×10^{-10} amperes was observed by reversing the polarity of the primary column so it delivered negative ions and electrons and using maximum offset of the "Z" electrode in the duoplasmatron. The extremely high current density in the negative polarity beam (150 ma/cm²) shows that the column was very efficiently transmitting electrons as well as negative ions.

If you assume a duoplasmatron ion source brightness of 100 amps/cm².ster in the positive mode which is our specification for the duoplasmatron and a spherical aberration coefficient of 23 cm for the objective lens, the theory which excludes all

other perturbations to the beam except spherical aberrations predicts a current of 2.78×10^{-11} amps in a spot of 0.34 in microns. Our measured value comes within 70% of the most optimistic theoretical value from the standpoint of possible aberrations to the beam. The actual measurement was not done with optimum settings on the condenser lenses. We feel this result is most encouraging and is indicative of the ability of the system to achieve better spot sizes than we have observed during our brief period of testing.

During the negative polarity ion beam tests the adjustable "Z" electrode in the duoplasmatron worked as predicted with only very marginal deterioration of the overall vacuum while the electrode was actually being moved.

As mentioned earlier the astigmator was not put into operation as we did not feel we had reached the point where astigmatism was our limiting factor.

5D(3). Secondary Ion Column and Secondary Electron Detector

The measurements of secondary ion transmission were made with the sample at 15 kV which means the primary column was at 13.5 to 14.5 kV and the lenses and duoplasmatron were at potentials as high as 35 kV. As a result, it was impossible to use the primary sweep system and current monitor. Under these conditions, the primary column would be set up as close as possible to a known operating point. The ion current leaving the secondary column was restricted by an angular aperture meeting the required specifications of the mass spectrometer and the secondary beam passing this aperture was collected by a faraday cup. Estimates of the value of the secondary ion current collected by the pickup electrode was made by using the grounded portions of the immersion lens, slit, and secondary electron detector deflection plates as a large faraday cup.

This latter measurement gave values which could only be considered upper limits due to the secondary electrons being lost across the immersion lens. All measurements of secondary ions were done with positive polarity on both primary and secondary beams to minimize electron effects on the measurement. An aluminum sample and air in the duoplasmatron were used in all cases.

One example of performance showed 1.1×10^{-10} amps of secondary ions exiting to the mass spectrometer with $< 4.8 \times 10^{-10}$ amps being collected by the secondary ion pickup electrode. This current was observed for all three of the larger slit openings with the restricted slit height. The smallest opening was not usable on this measurement due to a malalignment of range of the slit motion. The primary beam striking the sample in this case was estimated to be on the order of 2×10^{-7} amps.

On another occasion, the transmitted secondary current was observed to be 2.2×10^{-11} amps through the smallest slit for an efficiency of $> 13\%$ and 3.6×10^{-11} amps through the next to the smallest slit for an efficiency of $> 21\%$.

The secondary electron detector tests were made with the secondary ion slit with the largest opening. The best signal was observed at a detector voltage of 13 to 14 kV rather than the nominal design voltage of 20 kV. This was due to an easily corrected misalignment between the scintillator mounted from the vacuum chamber wall and the deflection plates suspended from the primary column mounting tube. In spite of this minor problem, signals of 2.5×10^7 Hz were observed with an estimated primary beam onto the sample of 5×10^{-11} amps of positive air ions. This signal was observed with a photomultiplier gain and discriminator setting which resulted in zero background counts when the primary beam was turned off but with all other voltages in the system left on.

During the secondary column tests it was necessary to shut off the ion pump immediately below the secondary column to eliminate background currents from the unbaffled pump.

6. CONCLUSIONS

The results of the unit obtained in a very short period of operation were very encouraging and show good promise for improved performance in the future. The unit showed outstanding reliability and stability throughout the testing period.

7. ACKNOWLEDGEMENT

This research was supported by the Advanced Research Projects Agency of the Department of Defense and was monitored by HQ USAF (AFTAC/TRE) Patrick Air Force Base, Florida 32925 under Contract #F33657-72-C-0632.

8. GLOSSARY OF ABBREVIATIONS

- AIM Advanced Ion Microprobe
- AMS Advanced Mass Spectrometer
- ARL Applied Research Laboratories
- IMMA Ion Microprobe Mass Analyzer^(R)
- RGA Residual Gas Analyzer
- VNC Vallecitos Nuclear Center